

Multisite Analyses of Spectral–Biophysical Data for Corn

C. L. Wiegand and A. H. Gerbermann

USDA, Agricultural Research Service, Subtropical Agricultural Research Laboratory, Remote Sensing Research Unit, Weslaco, Texas

K. P. Gallo

USDC, National Oceanographic and Atmospheric Administration, NESDIS, Applications Branch, EROS Data Center, Sioux Falls, South Dakota

B. L. Blad

Department of Agricultural Meteorology, University of Nebraska, Lincoln

D. Dusek

USDA, Agricultural Research Service, Conservation and Production Research Laboratory, Bushland, Texas

Reflectance factors and biophysical plant measurements for corn (*Zea mays* L.) experiments conducted at Bushland, Texas (102.2°W, 35.2°N), Tryon, Nebraska (100.8°W, 41.6°N), W. Lafayette, Indiana (87.0°W, 40.5°N) and Weslaco, Texas (98.0°W, 26.2°N) were fit by various equation forms for four of the most used vegetation indices (VI): *n*-space greenness (GVI), normalized difference (NDVI), perpendicular (PVI), and near-infrared to red ratio (RVI). The objective was to produce relations from the data pooled across all locations that could be recommended for general use for corn. Data were analyzed by premaximum leaf

area (pre- L_{max}), post-maximum leaf area (post- L_{max}), and whole season portions of the growing season. The vegetation indices ranked in descending order: GVI, PVI, NDVI, and RVI based on coefficients of determination (R^2), root mean square error (RMSE) in estimating leaf area index (L), and robustness across locations, soils, sun angles, cultivars, and radiometers. The power form was as good as any other equation form for the two-band vegetation indices, but quadratic and exponential equation forms were better for the three- or four-band GVI. Fractional absorbed photosynthetically active radiation (FPAR) was described for the combined data from Weslaco (PVI) and West Lafayette (GVI) by $FPAR = 0.0088 + 0.0315 (PVI, GVI) (R^2 = 0.94, RMSE = 0.07)$ and $FPAR = 1 - \exp[0.400(L / \cos Z)]$ ($r^2 = 0.95, RMSE = 0.04$), where Z is sun zenith angle. We conclude that the corn canopies characterized by green leaf area index so dominated the reflectance factor, hence VI

Address correspondence to Dr. C. L. Wiegand, USDA Agricultural Res. Serv., Remote Sens. Res. Unit, 2413 E. Highway 83, Weslaco, TX 78596-8344.

Published as Journal Series No. 9218, Agricultural Division, University of Nebraska.

Received 14 February 1990; revised 9 May 1990

observations, that it was possible to develop general relations for estimating L and FPAR for corn from VI measured in widely separated experiments.

INTRODUCTION

Current and prospective users of remote observations of economically important crops and other ecosystems need spectral-biophysical functional relations that hold across experiments and environments. However, most literature reports describe experiments in which one or more cultivars of one crop species were studied at one location for one or more crop seasons. In a few instances comparisons have been made for three or more species at one location (Dusek and Musick, 1986; Redelfs et al., 1987; Wiegand and Richardson, 1987; Wanjura and Hatfield, 1988), but results are not readily comparable because the same plant and spectral parameters were not measured and equation forms employed were nonuniform.

Comparisons among sites are even more difficult. Not only are data often proprietary but the interlocation variation increases due to differences in sun zenith angle (latitude, planting date, and time of day of observations), soil and surface conditions, instrument and measurement techniques, canopy architecture (leaf angle, canopy openness, and height), and cultural practices (row spacing, plant population, and fertilization).

Although radiative transfer models such as SAIL (Verhoef, 1984; Goel, 1988) are excellent for explaining systematically controlled variation, they are less able to summarize seasonal data where sources of variation are poorly known. For all the above reasons, equations that hydrologists, agricultural meteorologists, ecologists, plant breeders, plant growth and yield modelers, and other prospective users need are lacking.

To help provide the needed relationships, the Spectral-Agronomic Multisite-Multicrop Analyses (SAMMA) Project (Wiegand and Hatfield, 1988) was initiated. Under SAMMA, reflectance data from handheld and boom-mounted spectroradiometers and agronomic or biophysical plant measurements have been pooled across locations for uniform analyses of wheat (*Triticum aestivum* L.), corn (*Zea mays* L.), grain sorghum (*Sorghum bicolor* Moench), soybean (*Glycine max* Merr.),

cotton (*Gossypium hirsutum* L.), and alfalfa (*Medicago sativa* L.). In this paper, the spectral reflectance and biophysical data for corn experiments (Table 1) conducted at Bushland, Texas, Tryon, Nebraska, West Lafayette, Indiana, and Weslaco, Texas were analyzed using the same equation forms, first among treatments and years within locations and then among locations. The objectives were to determine statistically appropriate empirical relations within and among locations, and to summarize the general relations found.

METHODS AND MATERIALS

Data from four locations (Table 1) were pooled from experiments described elsewhere (Dusek and Musick, 1985; Gallo et al., 1985; Gallo and Daughtry, 1986; Mass et al., 1985; Wiegand and Richardson, 1987). Three locations provided reflectance factors for wet and dry soil and each treatment in corn plantings for each band of each instrument used (Table 2), while one location (W. Lafayette) provided vegetation indices (VI) directly.

Field experiments and biophysical measurements. Plant populations, dates of cardinal phenologic events, fertilization, maximum leaf area index (L_{\max}) achieved, cultivars used, grain yields, and treatments imposed are summarized in Table 1. At all locations row spacing was 0.76 m. Row direction was N-S at Bushland, Tryon, and West Lafayette, and E-W at Weslaco.

Green leaf area index (L , m^2/m^2) was determined by excising leaves at the ligule from a sample of two to five plants per replication, passing them through an area meter, and expanding the area of leaves based on plant population to that per m^2 of ground area. However, the large number of treatments at Bushland, and Tryon, permitted acquisition of L from only part of the treatments and those on a staggered schedule. Some treatments for Bushland were deleted because observations were insufficient to establish seasonal trends and for both these locations the L data were smoothed by either manual graphical or exponential polynomials of time (Hughes and Freeman, 1967; Wiegand et al., 1989) machine procedures. Leaf area data for West Lafayette and Weslaco were used as provided summarized by treatment.

Above-ground fresh and dry phytomass (FM, DM, g/m^2) and fresh and dry leaf mass (FLM,

Table 1. Treatments, Cultivars, and Growth Characteristics of Corn in the Experiments of This Study

Location; Lat., Long.	YEAR	Treatments Used	CULTIVARS	Plant Population (no. / m ²)	Phenology (DOY)				Grain Yield ^a (kg / ha)	Fertilizer (kg / ha)
					<i>L</i> _{max}	Emergence	Silking	Black Layer		
Bushland, TX; 102.2°W, 35.2°N	1982	irrigation sequences 1, 2, 3, 4 & 8	Pion. 3184	6.2	1-4.1	133	207	251	8350	N-220
				6.5	2-4.0	133	207	251	9650	P-0
				6.0	3-3.6	133	207	251	1600	K-0
				6.2	4-4.1	133	207	251	8700	
				6.2	8-4.1	133	207		10900	
	1983	irrigation sequences 1, 2, 4 & 8	Pion. 3184	6.3	1-3.9	157		—	5410	N-220
				6.6	2-3.1	157		—	4620	P-0
				6.2	4-3.6	157		—	4600	K-0
				6.3	8-3.7	157		—	5130	
Tryon, NB; 100.8°W, 41.6°N	1984	full & partial irrig.; full & half pop.	Pion. 3901	7.5	F-4.9	144	212	272	8150	N-176
			Pion. 3901	7.5	P-4.0	144	212	272	5600	P-0
			B73XM017	8.0	F-5.1	144	219	280	7200	K-0
			B73XM017	7.3	P-4.3	144	219	280	2700	
			Pion. 3901	4.6	F-3.4	144	212	272	7300	
			Pion. 3901	4.1	P-2.4	144	212	272	4100	
W. Lafayette, IN; 87.0°W, 40.5°N	1982	two pl. dates; two pops.	Adlers 30X	5.0	3.9	141	210	260	10800	N-200
				10.0	7.1	141	210	260	13200	P-53
				5.0	3.6	179	230	280	5620	K-100
				10.0	6.3	179	230	280	7507	
Weslaco, TX; 98.0°W, 26.2°N	1985	irrigated; nonirrig.	Asgrow 405	8.2	I-3.9	147	200	240	4060	N-0
				8.2	D-3.7	147	200	233	1950	P-0 K-0

^aOven dry basis.

Table 2. Instruments, Wavelengths, and Their Use by Experimental Sites

Bushland, Tryon MMR 12-1000		Tryon, W. Lafayette EXOTECH 100		Weslaco MARK II	
Band	μm	Band	μm	Band	μm
1	0.45–0.52				
2	0.52–0.60	1	0.50–0.60		
3	0.63–0.69	2	0.60–0.70	1	0.63–0.69
		3	0.70–0.80		
4	0.76–0.90	4	0.80–1.10	2	0.76–0.90
5	1.15–1.30				
6	1.55–1.75				
7	2.08–2.35				

LM, g/m²) were provided for Bushland, and Tryon, while fraction of photosynthetically active radiation absorbed (FPAR) (Gallo and Daughtry, 1986) was provided from West Lafayette and Weslaco.

Reflectance factors and vegetation indices. Bidirectional reflectance factor measurements (Richardson, 1981; Jackson and Moran, 1987) were acquired with Barnes Modular Multiband 12-1000 Radiometers (MMR, Robinson et al., 1979) at two sites, Exotech 100 (EXO) radiometers at two sites, and a Mark II radiometer (Tucker et al., 1981) at

one site (Table 2). At Tryon, measurements were made on the same dates with both MMR and EXO instruments. MMR and EXO instruments had fields of view of 15°, were boom-mounted, and measurements were made looking vertically downward from 5 m to 8.5 m above the ground. The 24° field of view Mark II instrument used at Weslaco was handheld and measurements were made from 1 m to 1.5 m above the canopy centered over the plant row.

Four of the commonly used vegetation indices, greenness (GVI, Kauth and Thomas, 1976; Jackson, 1983), perpendicular vegetation index (PVI, Richardson and Wiegand, 1977), normalized difference (NDVI, Rouse et al., 1974), and NIR/RED ratio (RVI, Tucker, 1979) were calculated from the reflectance factors and used for all within and across location analyses of *L* versus *VI*. In addition, a difference vegetation index, $DVI = MMR5 - MMR6$ (Shibayama and Akiyama, 1989) and a product ratio vegetation index, $PRVI = (MMR3 \times MMR4 \times MMR6) / (MMR1 \times MMR7)$ (Dusek et al., 1985) were calculated to examine relationships with FM, DM, FLM, and LM for the two locations with the required data. The soil line and

Table 3. Soil Line and Vegetation Index Equations by Location

Location	Radiometer	Soil Line (SL) and Vegetation Index Equations ^a	Eq. No.
Bushland	MMR	SL: MMR4 = 2.08 + 1.20 (MMR3)	(2)
		GVI = -0.329 (MMR2) - 0.622 (MMR3) + 0.710 (MMR4)	(3)
		PVI = 0.639 (MMR4) + -0.769 (MMR3) - 1.33	(4)
Tryon	MMR	SL: MMR4 = 1.93 + 1.26 (MMR3)	(5)
		GVI = -0.355 (MMR2) - 0.617 (MMR3) + 0.702 (MMR4)	(6)
		PVI = 0.62 (MMR4) - 0.784 (MMR3) - 1.10	(7)
	EXO	SL: EXO 4 = 3.07 + 1.36 (EXO2)	(8)
		GVI = -0.441 (EXO1) - 0.645 (EXO2) + 0.151 (EXO3) + 0.606 (EXO4)	(9)
W. Lafayette	EXO	PVI = 0.593 (EXO4) - 0.805 (EXO2) - 1.82	(10)
		SL: None	
		GVI ^b = -0.489 (EXO1) - 0.612 (EXO2) + 0.173 (EXO3) + 0.595 (EXO4)	(11)
Weslaco	Mark II	SL: MK2 = 3.49 + 1.18 (MK1)	(12)
		PVI = 0.647 (MK2) - 0.762 (MK1) - 2.26	(13)
All	Any	RVI = NIR/RED where NIR = MMR4, EXO4, MK2; RED = MMR3, EXO2, MK1	(14)
		NDVI = (NIR - RED)/(NIR + RED)	(15)

^aUsing bands as numbered in Table 2.^bFrom Rice et al., 1980.

vegetation index equations are given by locations and instruments in Table 3.

Data pairing. Biophysical plant measurements that were made at about 10-day intervals were summarized to treatment means and paired with treatment means of spectral measurements made within 2 days of the biophysical measurements. The data were divided into pre- L_{\max} , post- L_{\max} , and full growing season portions for particular analyses to deal with nonliving phytomass effects on observations (Wiegand and Hatfield, 1988). Data for the last date in the pre- L_{\max} portion was included as the first date in post- L_{\max} sets when analyzed separately, but data for the tie point were not repeated in the full season data sets.

Analysis procedures. Data were first analyzed within location by instrument and year to determine whether cultivars or agronomic management affected equation coefficients. SAS (SAS Institute, 1988) nonlinear procedures and the model form

$$Y = Ci\{1 - Ai \exp[-Bi(X)]\} \quad (1)$$

(Asrar et al., 1984; Best and Harlan, 1985) were used, where

Y = fractional PAR absorption (FPAR) or any of the four vegetation indices GVI, PVI, NDVI, or RVI,

X = green leaf area index L ,

Ci = the asymptotically limiting value of 'Y' at large L ,

Ai = transmission at $L = 0$ when FPAR is 'Y', (1-NDVI of bare soil) when 'Y' is NDVI, etc. (Wiegand and Hatfield, 1988),

Bi = an absorption-scattering coefficient for the wavebands used that is leaf angle distribution and solar zenith angle dependent,

i = a treatment identifier.

The following hypotheses were tested:

1. FM vs. RM1 = $CiAiBi$ vs. $CAiBi$; if significant, the C 's differ in Eq. (1);
2. RM1 vs. RM2 = $CAiBi$ vs. $CABi$; if significant, the A 's differ in Eq. (1);
3. RM2 vs. RM3 = $CABi$ vs. CAB ; if significant, the B 's differ in Eq. (1).

In hypotheses 1, 2, and 3, above, the full model (FM) symbolized by $CiAiBi$ means C , A , and B are each unique for each treatment; the model reduced by one parameter (RM1) symbolized by $CAiBi$ means the C is common among treatments but A and B are unique for each treatment; the model reduced by two parameters (RM2) symbolized by $CABi$ means C and A are common for all treatments but B is unique for each. If none of the tests is significant, the fully reduced model (RM3) applies; that is, all treatments can be represented by a common set of C , A , and B coefficients.

Significance of hypotheses was determined by an asymptotic F -test:

$$F_{(Hi)} = \frac{N - \text{PFM}}{\text{PFM} - \text{PRM}} \times \frac{\text{RSS (model reduced by } Hi) - \text{RSS(Full model)}}{\text{RSS(full model)}}$$

where

N = the number of observations,

PFM = the number of parameters in the full model of the hypothesis tested (the one on the left in each hypothesis statement above),

PRM = the number of parameters in the reduced model (the one to the right of "vs." in each hypothesis statement)

For example, for three treatments, PFM = 9, PRM1 = 7, PRM2 = 5, and PRM3 = 3.

Intralocation analyses were also performed using $L/\cos Z$ as 'X' in Eq. (1), where Z is the solar zenith angle to learn whether L or $L/\cos Z$ gave lower residual sums of squares. For these comparisons, the data sets for Tryon and Weslaco contained the solar zenith angles at the time of the spectral measurements whereas for Bushland and West Lafayette they were calculated for solar noon on measurement dates from ephemeris equations since spectral observations had been acquired within about an hour of solar noon.

Because of the availability of spectral observations, especially those from LANDSAT, SPOT, and NOAA polar orbiting satellites and the need for biophysical parameter estimates from these observations, we also used linear, quadratic, power, and two-parameter exponential equations in which VI was the independent and the plant biophysical parameters and FPAR were the dependent variables. These equations were determined for data pooled across locations for pre- L_{\max} , post- L_{\max} , and full season data sets.

RESULTS

Figure 1, in which L , DM, NIR, and RED reflectance factors are presented for each location and subexperiment versus day of year (DOY), indicates that the plant canopies developed very similarly at Bushland in 1982 and Tryon in 1984. Late planting at Bushland in 1983 (due to weather) compared with 1982 and at West Lafayette (by design) resulted in lower L than earlier plantings. Rate of dry matter increase was about the same at all locations from DOY 200 to DOY 220. Re-

flectance factors in the RED were more uniform than in NIR. At Weslaco, use of the instrument close to the canopy and centered over the plant row cannot simultaneously account for high NIR and high RED reflectance factors because they respond oppositely to soil and green vegetation. For this study the Weslaco data were represented using a lower reflectance of the reference panels taken to the field, based on calibration against a newly acquired halon reference panel, than in results reported by Wiegand and Richardson (1987).

Within Location Analyses

Vegetation Indices

The relation between L (graphed as the dependent variable) and the four vegetation indices GVI, NDVI, PVI, and RVI are shown in Figure 2 by location for the pre- L_{\max} portion of the growing season. Observations are shown as open symbols and the statistical fit to Eq. (1) by closed or solid symbols. For Tryon, only the MMR data are displayed. It is evident that NDVI and GVI have the least scatter among locations. The MMR data for Bushland and Tryon are closely coincident in GVI, NDVI, and RVI up to about $L = 3$. GVI and NDVI for the West Lafayette EXO data agreed well with the MMR data for Bushland and Tryon but gave a larger RVI. The data from Weslaco (Mark II radiometer) fall between the other data sets in NDVI up to $L = 2$, but have higher PVI and lower RVI at a given L in keeping with the high NIR and RED reflectance factors in Figure 1.

The within-location analyses were conducted to learn whether agronomic treatments caused the coefficients C , A , and B in Eq. (1) to differ statistically. Briefly, results by location were:

Bushland. For the 1982 data, C , A , and B were the same for all treatments in all VI. For 1983, C and A were the same but B differed among treatments for all VI. For the combined 1982 and 1983 data, C , A , and B were the same for GVI and PVI, but the values of B differed among treatments for NDVI and RVI.

Tryon. For both the MMR and EXO data, C and B differed among treatments for GVI and PVI

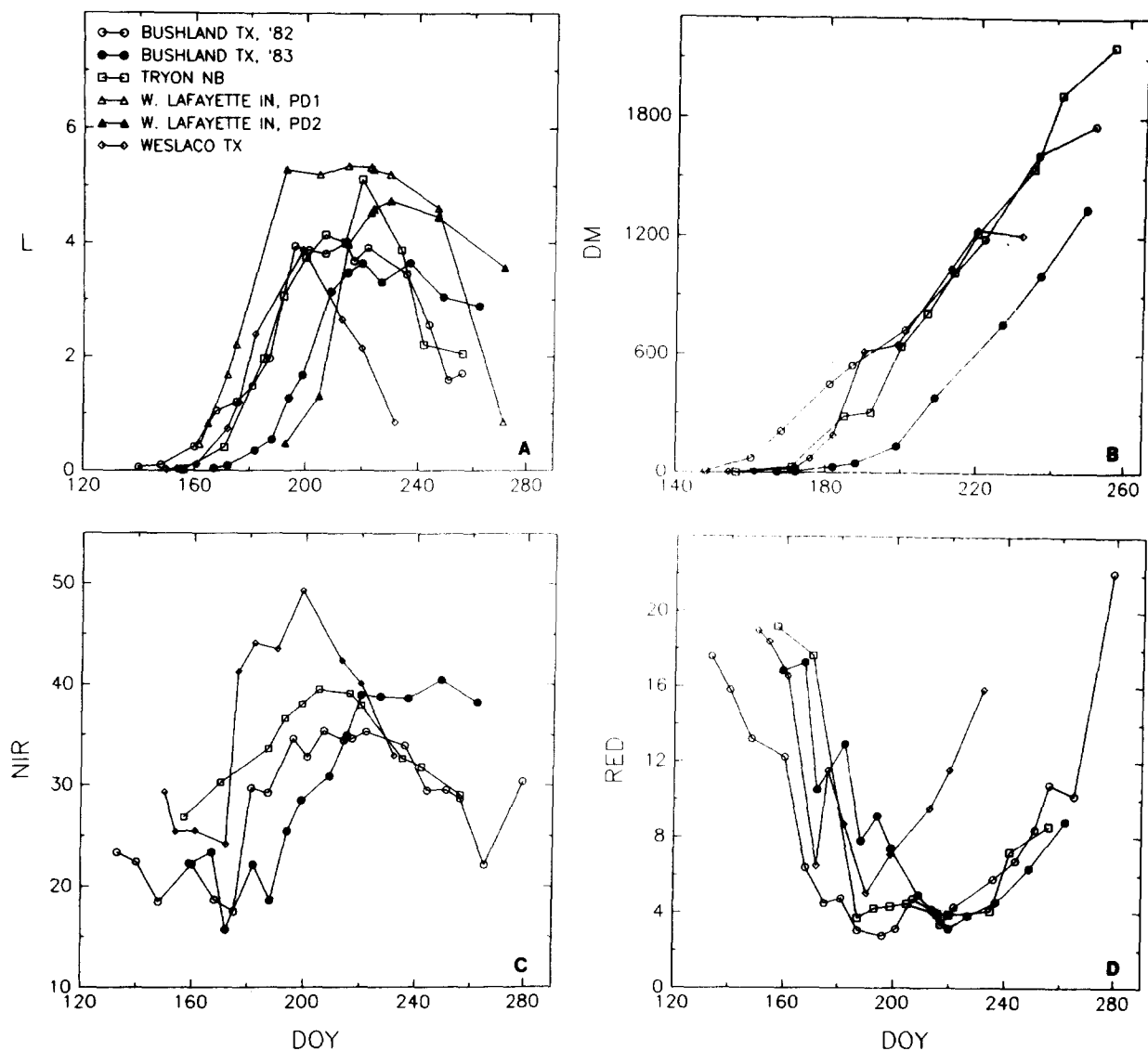


Figure 1. Seasonal leaf area index (L), above-ground dry phytomass (DM), near-infrared (NIR), and visible red (RED) reflectance factors for each location and subexperiment of this study. DOY is day of year.

whereas B differed among treatments for $NDVI$ and RVI . This same result for both radiometers indicates that differences in L among treatments were mainly responsible.

West Lafayette. Populations and planting dates did not cause C , A , and B to differ for GVI and $NDVI$, but B differed by population for RVI . For all locations the residuals were large for RVI at low LAI ; this VI is affected by the amount of soil in the line-of-sight of the instrument and by its water content.

Weslaco. C , A , and B did not differ between irrigation treatments for the three VI that could be calculated, PVI , $NDVI$, and RVI .

The above analyses indicate that the cultural treatments did not have a strong effect on the equation coefficients. However, in three of the experiments irrigation was the main treatment and L did not differ greatly between irrigated and nonirrigated treatments during the pre- L_{max} portion of the growing season (Table 1). A probable source of variation of greater importance was experimental error in the measurements of L , especially in the L range 2–4, that we attribute to undersampling of L (too few subsamples, or too few or nonrepresentative plants in subsamples). This source of variation and that associated with use of different cultivars having different canopy

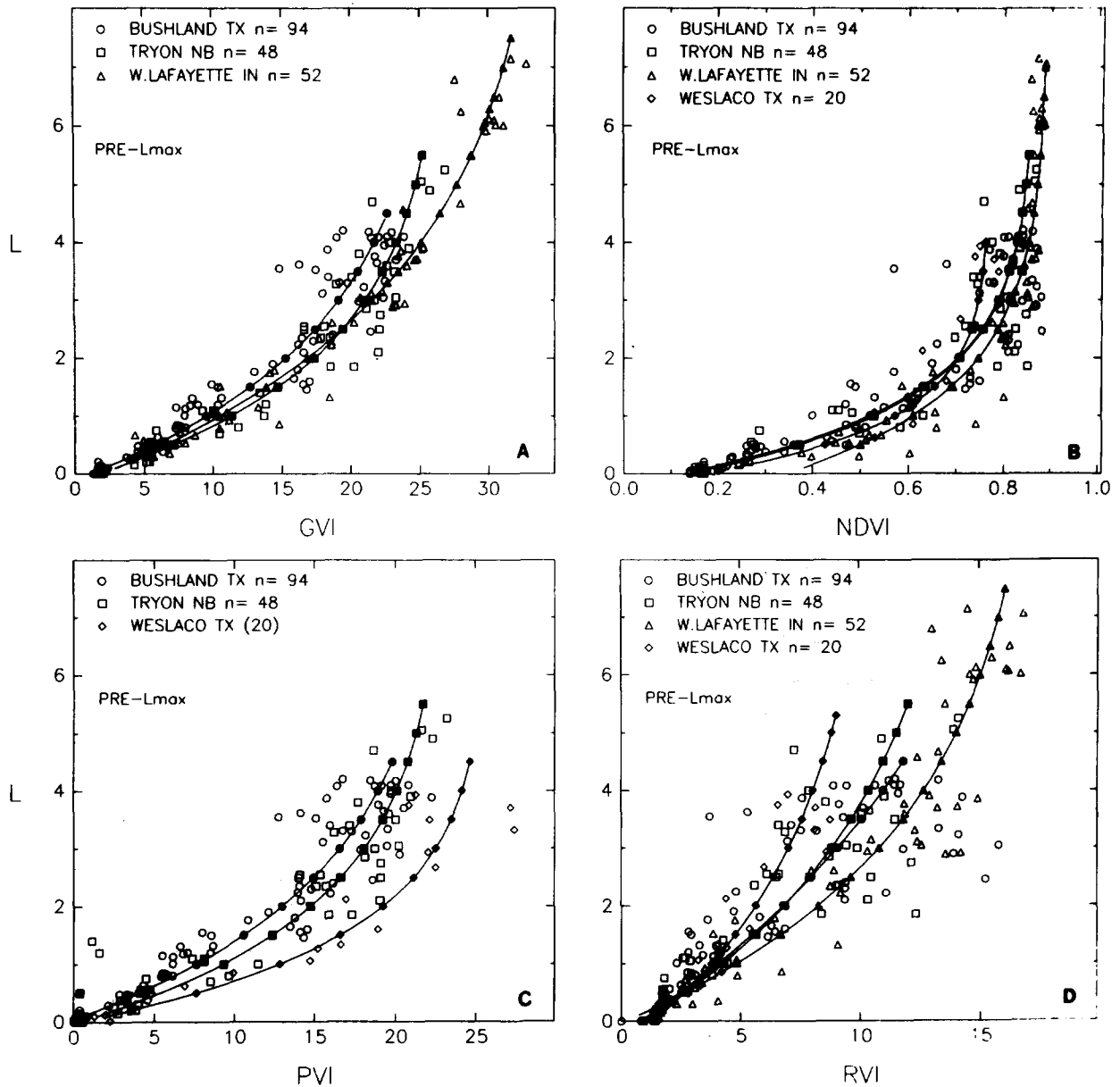


Figure 2. Relation between L and the vegetation indices GVI, NDVI, PVI, and RVI for the pre- L_{max} portion of the growing season as fit by the fully reduced form of Eq. (1) by location.

architectures contribute to uncontrolled variation in this study.

Another source of variation in the data is solar zenith angle (Z). In Figure 3, observed L is plotted versus $L\cos Z = L/\cos Z$ for pre- L_{max} and post- L_{max} portions of the season. The pre- L_{max} portion of the season at all locations surrounded the long days of June (21 June = DOY 172) so that deviation from the 1:1 line was small. Deviations were somewhat larger for the post- L_{max} portion of

the season and increased as days shortened toward the end of the season. (The large deviations for Tryon are for two dates when early morning observations were used because that was the only time of day when all treatments were observed.) Also, 12 comparisons were made between residual sums of squares for the VI estimated first from L and then from $L/\cos Z$ using identical forms of Eq. (1). The residual sums of squares were slightly larger (1–5%) for $L/\cos Z$ in all except one in-

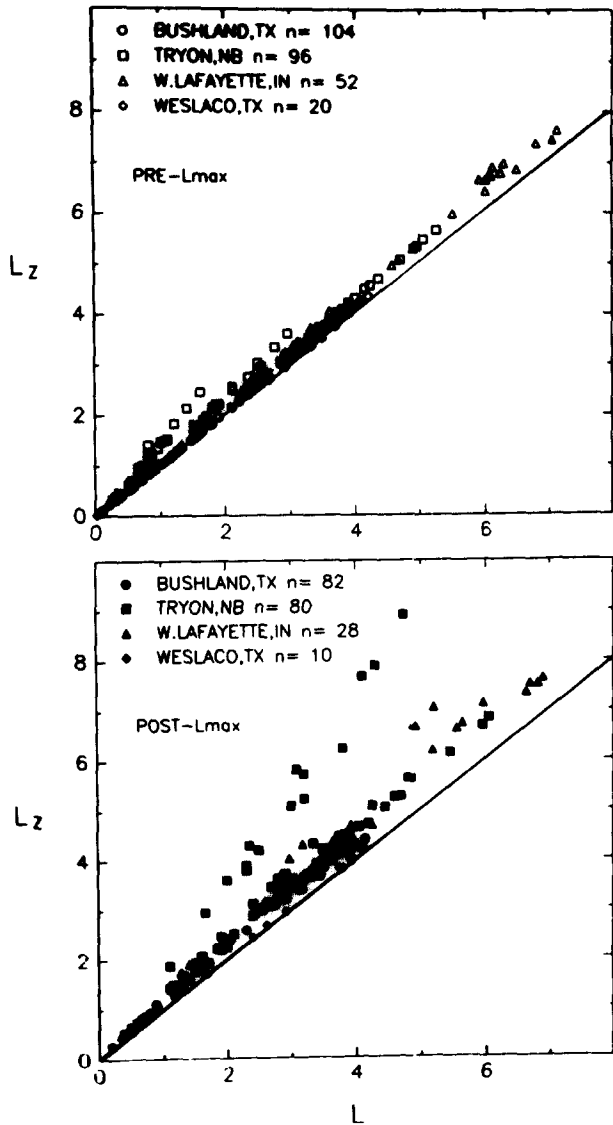


Figure 3. Relation between L and $L_z = L / \cos$ solar zenith angle for pre- L_{\max} and post- L_{\max} portions of the growing season by location.

stance—for NDVI in the West Lafayette data set. Based on the approach used solar zenith angle was a minor source of variation in VI observations in this study. [Note: Reviewers suggested adjustment of RED and NIR reflectance factors for zenith angle before calculating vegetation indices but we lacked the parameter information and method, such as the scattering by arbitrarily inclined leaves (SAIL) model (Verhoef, 1984; Goel, 1988) to do it. Our viewpoint was that the reflectance factor measurements themselves contained the zenith angle responses and that L needed to be adjusted in proportion to path length through the canopy to be compatible with them. Although our method was a

simple one, it should have been adequate to determine whether zenith angle had a very strong effect or not.]

Fractional PAR Absorbed

Application of Eq. (1) to the West Lafayette FPAR data gave $C = 1.031 \pm 0.034$, $A = 1.010 \pm 0.032$, $B_5 = 0.426 \pm 0.042$, and $B_{10} = 0.365 \pm 0.041$, where the 5 and 10 on B refer to 5 and 10 plants/ m^2 , respectively. That is, C (asymptotically approached value of FPAR as L approaches infinity) and A (light transmission at $L = 0$) did not differ from unity, whereas B (scattering coefficient in the PAR wavelengths) differed between populations. Planting date did not affect the coefficients.

For the Weslaco FPAR data, $C = 0.851 \pm 0.032$, $A = 1.00 \pm 0.025$, and $B = 0.597 \pm 0.066$. Thus, irrigation treatment did not affect the coefficients and A was not different from unity. C was lower for Weslaco than for West Lafayette because observed L_{\max} and FPAR_{\max} (decimal fraction) were much lower at 3.9 and 0.78 at Weslaco compared with 7.1 and 0.95 at West Lafayette.

Among Location Analyses

The data pooled for all sites are summarized in Figure 4 and the equations and statistical parameters for the pre- L_{\max} , post- L_{\max} , and whole season periods as analyzed separately are given in Tables 4, 5, and 6, respectively. The modular radiometer (MMR) data for Tryon, Nebraska, were used throughout these analyses; the observed L were common for both MMR and EXO measurements and the use of these same data twice would be inappropriate. In Figure 4, the nonpower form equations that gave the highest coefficient of determination (R^2) and their fits to the pre- and post- L_{\max} seasonal portions are displayed. The best fit for GVI was quadratic, for NDVI exponential, and for PVI and RVI linear. However, the PVI data set did not contain the 80 observations for West Lafayette, which contained the highest LAI; had it, the best fit for PVI would likely have been quadratic also since PVI and GVI are highly correlated.

Statistical t -tests for the linear equations for RVI and PVI in Figure 4 showed that the slopes did not differ for RVI but did for PVI. For PVI the intercepts for none of the three periods differed

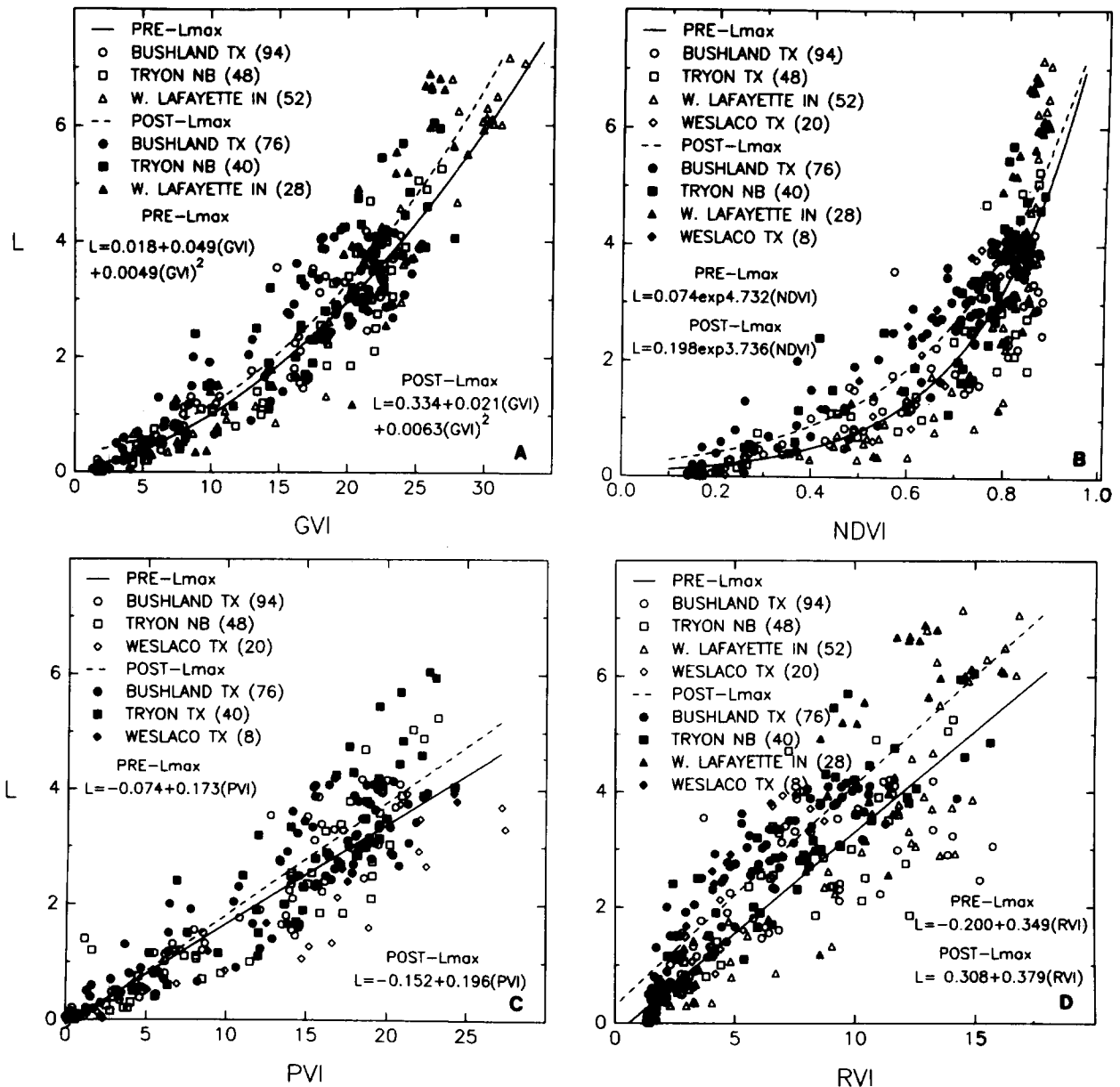


Figure 4. Data for all locations pooled and equations that describe the data by pre- L_{\max} (open symbols) and post L_{\max} (closed symbols) portions of the season.

from zero, whereas the pre- and post- L_{\max} intercepts differed from zero for RVI but the intercept for the whole season did not. Thus Eq. (18b) in Table 6 can represent the seasonal RVI data. The root mean square error (RMSE) for estimating L from Eq. (18b) was 0.86, somewhat higher than for fractional seasonal portions [see Eqs. (18) and (18a), Tables 4 and 5, respectively].

The quadratic equation for estimating L from GVI accounted for 92.8% of the variation and estimated L with a RMSE of 0.49 as shown in Table 4 [Eq. (24)]. An F -test showed that the

quadratic term did not contribute significantly to the fit for PVI during any seasonal period, but did contribute significantly for each of the other three indices during the post- L_{\max} and whole season periods.

The exponential and power equations [Table 4, Eqs. (23) and (31), respectively] best described the NDVI data. The exponential equation estimated L from NDVI with a RSME of 0.79 for both the pre- L_{\max} and post- L_{\max} periods, and 0.84 for the whole season. The slopes (4.732 versus 3.736) were highly significantly different for NDVI

Table 4. Across Location Equations for the Pre- L_{\max} Portion of the Growing Season

Equations (by Form)	R^2 ^a	RMSE	S_b	Eq. No.	
1. LAI = $-0.604 + 0.191(\text{GVI})$.89	.60	.005	(16)	
= $-0.074 + 0.173(\text{PVI})$.85	.58	.006	(17)	
= $-0.200 + 0.349(\text{RVI})$.81	.78	.012	(18)	
= $-1.311 + 5.746(\text{NDVI})$.71	.98	.253	(19)	
2. LAI = $0.486 \exp 0.086(\text{GVI})$.90	.57	.003	(20)	
= $0.587 \exp 0.086(\text{PVI})$.77	.72	.005	(21)	
= $0.742 \exp 0.132(\text{RVI})$.74	.93	.006	(22)	
= $0.074 \exp 4.732(\text{NDVI})$.81	.79	.295	(23)	
3. LAI = $0.018 + 0.049(\text{GVI}) + 0.0049(\text{GVI})^2$.93	.49	—	(24)	
= $-0.036 + 0.157(\text{PVI}) + 0.0008(\text{PVI})^2$.85	.58	—	(25)	
= $-0.403 + 0.437(\text{RVI}) - 0.0057(\text{RVI})^2$.82	.78	—	(26)	
= $0.810 - 5.678(\text{NDVI}) + 11.099(\text{NDVI})^2$.79	.82	—	(27)	
4. LAI = $0.023(\text{GVI} * * 1.633)^b$.78	.85	.096	(28)	
= $0.120(\text{PVI} * * 1.117)$.85	.58	.074	(29)	
= $0.293(\text{RVI} * * 1.048)$.81	.79	.053	(30)	
= $7.021(\text{NDVI} * * 3.351)$.80	.81	.240	(31)	
5. FPAR = $1 - 0.986 \exp(-0.416)(L)$.96	.05	.013	(36)	
= $1 - 0.959 \exp(-0.380)(L_z)$.96	.05	.012	(37)	
6. Fully reduced three-parameter model					
	C	A	B	R^2	RMSE
GVI	34.32 ± 1.43	$0.951 \pm .008$	$0.283 \pm .023$.95	2.05 (32)
PVI	23.46 ± 1.13	$1.007 \pm .015$	$0.477 \pm .051$.92	2.30 (33)
RVI	24.14 ± 4.2	$0.959 \pm .009$	$0.144 \pm .036$.84	1.89 (34)
NDVI	0.860 ± 0.01	$0.834 \pm .012$	$0.816 \pm .045$.94	0.07 (35)

^a(Total corrected sum of squares – residual sum of squares)/total corrected sum of squares. Applies also to Tables 5 and 6.

^bDouble asterisks mean “raised to the power” here and in Tables 5 and 6.

Table 5. Across Location Equations for the Post- L_{\max} Portion of the Growing Season

Equations (by Form)	R^2	RMSE	S_b	Eq. No.	
1. LAI = $-0.826 + 0.214(\text{GVI})$.76	.81	.010	(16a)	
= $-0.152 + 0.196(\text{PVI})$.77	.68	.009	(17a)	
= $0.308 + 0.379(\text{RVI})$.75	.80	.017	(18a)	
= $-1.681 + 6.922(\text{NDVI})$.68	.91	.373	(19a)	
2. LAI = $0.555 \exp(0.087)(\text{GVI})$.75	.46	.006	(20a)	
= $0.780 \exp(0.124)(\text{PVI})$.74	.47	.006	(21a)	
= $0.626 \exp(0.185)(\text{RVI})$.57	.59	.013	(22a)	
= $0.144 \exp(4.118)(\text{NDVI})$.77	.44	.178	(23a)	
3. LAI = $0.334 + 0.021(\text{GVI}) + 0.0063(\text{GVI})^2$.78	.76		(24a)	
= $0.087 + 0.143(\text{PVI}) + 0.0022(\text{PVI})^2$.77	.68		(25a)	
= $-0.235 + 0.572(\text{RVI}) - 0.0129(\text{RVI})^2$.77	.78		(26a)	
= $1.293 + 5.917(\text{NDVI}) + 11.554(\text{NDVI})^2$.75	.81		(27a)	
4. LAI = $0.028(\text{GVI} * 1.599)$.78	.77	.106	(28a)	
= $0.126(\text{PVI} * 1.138)$.77	.68	.087	(29a)	
= $0.587(\text{RVI} * 0.845)$.76	.79	.048	(30a)	
= $7.013(\text{NDVI} * 2.562)$.75	.81	.196	(31a)	
5. Fully reduced three-parameter model					
	C	A	B	R^2	MSE
GVI	29.01 ± 1.56	0.923 ± 0.027	0.342 ± 0.047	.84	2.71 (32a)
PVI	25.32 ± 1.83	1.012 ± 0.036	0.372 ± 0.061	.83	2.59 (33a)
RVI	36.58 ± 19.3	0.984 ± 0.01	0.069 ± 0.045	.76	1.83 (34a)
NDVI	0.901 ± 0.027	0.814 ± 0.028	0.492 ± 0.056	.82	0.08 (35a)

Table 6. Across Location Equations for the Whole Season (Combined Pre- and Post- L_{\max} Portions of the Season)

Equations (by Form)	R^2	RMSE	S_b	Eq. No.
1. LAI = $-0.656 + 0.200(\text{GVI})$.84	.71	.005	(16b)
= $-0.090 + 0.183(\text{PVI})$.83	.64	.005	(17b)
= $-0.018 + 0.365(\text{RVI})$.77	.86	.010	(18b)
= $-1.417 + 6.184(\text{NDVI})$.70	.96	.211	(19b)
2. LAI = $0.554 \exp(0.083)(\text{GVI})$.85	.71	.002	(20b)
= $0.665 \exp(0.083)(\text{PVI})$.76	.74	.004	(21b)
= $0.991 \exp(0.118)(\text{RVI})$.68	1.01	.005	(22b)
= $0.127 \exp(4.162)(\text{NDVI})$.78	.84	.198	(23b)
3. LAI = $0.009 + 0.061(\text{GVI}) + 0.0048(\text{GVI})^2$.87	.65	—	(24b)
= $-0.031 + 0.162(\text{PVI}) + 0.0009(\text{PVI})^2$.83	.64	—	(25b)
= $-0.483 + 0.551(\text{RVI}) - 0.0123(\text{RVI})^2$.78	.83	—	(26b)
= $0.742 - 4.763(\text{NDVI}) + 10.464(\text{NDVI})^2$.77	.98	—	(27b)
4. LAI = $0.027(\text{GVI} * 1.596)$.87	.65	.054	(28b)
= $0.129(\text{PVI} * 1.112)$.83	.63	.058	(29b)
= $0.421(\text{RVI} * 0.936)$.77	.86	.038	(30b)
= $6.866(\text{NDVI} * 2.872)$.77	.85	.158	(31b)

during the pre- and post- L_{\max} seasonal periods. Standard error of the slope (S_b) was approximately proportional to the slope.

The power equation form gave as good a fit for PVI, RVI, and NDVI as any of the other equations during all three seasonal periods [Eqs. (29), (30), and (31) of Tables 4, 5, and 6]. This is a versatile equation form that describes all the two-band VI reasonably well. However, it does not describe the three- and four-band greenness vegetation indices (see Table 3) well; for them the quadratic and exponential expressions are superior. For the pre- L_{\max} seasonal portion, the RMSE in estimating L from GVI was 0.49 for the quadratic, 0.57 for the exponential, and 0.85 for the power expressions, respectively.

The coefficients for the three parameter (or coefficient) model for estimating the VI from L are shown in the last section in Tables 4 and 5. For the pre- L_{\max} period this equation form accounted for 95.0% and 93.9% of the variation in GVI and NDVI, respectively, and estimated GVI with a RMSE of 2.05 and NDVI with a RMSE of 0.07 [Table 4, Eqs. (32) and (35)]. The three-parameter model also explained more of the variation in the data for the post- L_{\max} portion of the season than did any of the other equation forms [Table 5, Eqs. (32)–(35)]. Fits were even better for individual locations shown in Figure 2, where the independent and dependent variables have been interchanged compared with Eq. (1), since users will want to estimate L from VI, not VI from L .

The fractional PAR absorbed is expressed as a function of L and L_z in the customary form by Eqs. (36) and (37) of Table 4. The extinction coefficient depends on both Z and leaf angle distribution, so that use of L_z makes extinction coefficients obtained at different sites that differ in latitude and growing seasons more comparable. In this study measurements were made in summer when the sun zenith position was close to nadir so that the equation coefficients were not affected much. For the combined data for Weslaco and W. Lafayette, the fully reduced Eq. (1) gave

$$\text{FPAR} = 1 - \exp[-.400(L_z)],$$

$$r^2 = .954, \quad \text{RSME} = 0.042, \quad (38)$$

since C and A did not differ from unity.

Many users also want to estimate FPAR from vegetation indices. The combined data from West Lafayette (GVI) and Weslaco (PVI) gave the linear relation

$$\text{FPAR} = 0.0088 + 0.0315(\text{PVI}, \text{GVI}),$$

$$r^2 = 0.937, \quad \text{RMSE} = 0.070 \quad (39)$$

shown in Figure 5. Similarly, FPAR estimated from NDVI gave

$$\text{FPAR} = -0.488 + 1.525(\text{NDVI}),$$

$$r^2 = 0.889, \quad \text{RMSE} = 0.092. \quad (40)$$

If one can estimate FPAR from VI, it is not necessary to know L because one of L 's main uses is for FPAR estimation.

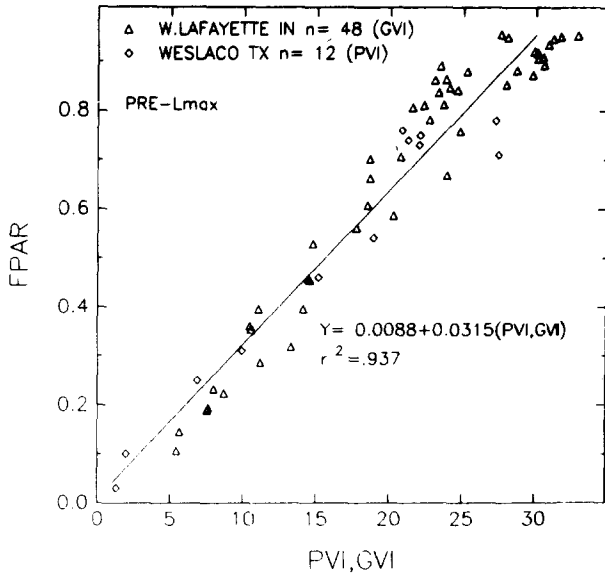


Figure 5. FPAR estimated from the combined GVI data from West Lafayette and PVI data from Weslaco.

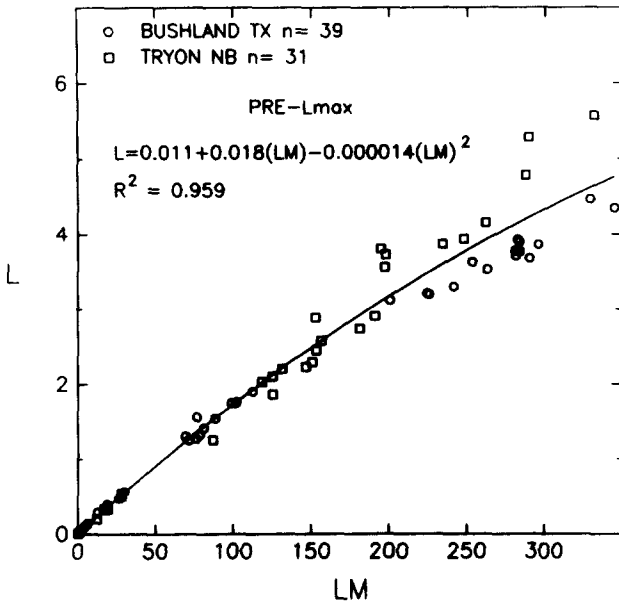


Figure 6. Relation between leaf mass (LM, g/m²) and leaf area index (L) for the combined data from Bushland and Tryon.

Leaf mass (LM, g/m²) can be determined more readily than leaf area index so that it is advantageous to develop a relation between LM and L and use it for further estimates of L. Figure 6 displays the relation

$$L = 0.011 + 0.018(LM) - 0.000014(LM)^2,$$

$$R^2 = 0.959, \quad RMSE = 0.29, \quad (41)$$

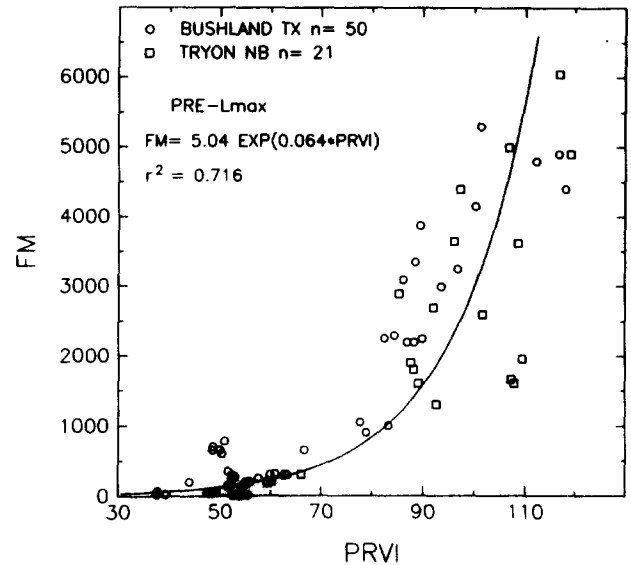
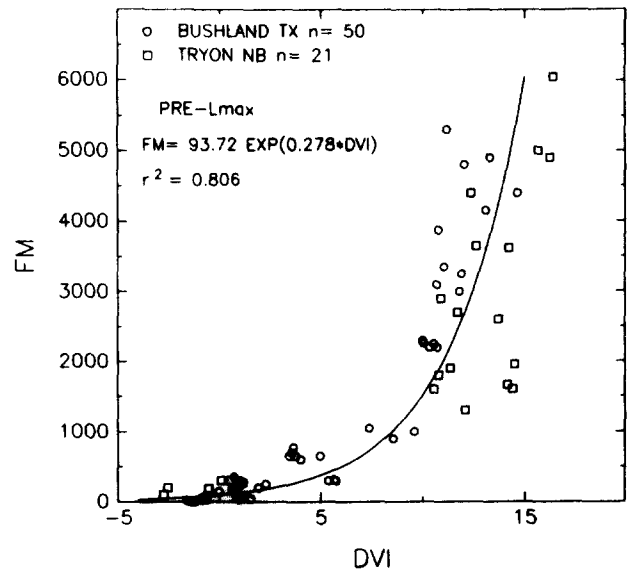


Figure 7. Difference vegetation index (MMR5 - MMR6) and product ratio vegetation index (MMR3 × MMR4 × MMR6) / (MMR1 × MMR7) versus smoothed above-ground fresh phytomass (FM, g/m²) for Bushland and Tryon.

developed for the pre- L_{max} period from the LM and L measurements provided from Bushland and Tryon. The quadratic term was statistically significant ($F = 13.7$).

In Figure 7, the difference vegetation index, $DVI = MMR5 - MMR6$, and the product ratio index, $PRVI = (MMR3 \times MMR4 \times MMR6) / (MMR1 \times MMR7)$, are related to fresh phytomass, FM (g/m²). Qualitatively, FM versus DVI had the same pattern in the observations but more scatter than FM versus NDVI (not shown). Similarly, FM versus PRVI had about the same pattern, but less

scatter than did FM versus GVI (not shown). The similarities mentioned were not expected because the bands differ so much. The relationships are so extensive that a separate paper in which they are explored more fully is merited. We conclude, however, that FM cannot be estimated as well from the MMR bands and the VI used in this study as could L . The broad bands of the MMR may be limiting because there are reports in the literature of coefficients of determination in excess of 0.9 between FM or DM and combinations of very narrow bands in the mid-infrared and near-infrared (e.g., Shibayama and Akiyama, 1989).

DISCUSSION

When we began working with the experimental data, we were concerned that the specific plants in the small samples for plant measurements (two to five plants per replicate, sometimes in only one replicate of each treatment) were not representative of the population observed by the radiometers. To reduce random experimental error, plant measurements were smoothed when paired with spectral observations, although smoothing had little effect on about 90% of the observations. Measurements of L , FM, DM, FLM, and LM on particular samples were internally consistent so that plant measurements paired with each other, as in Figure 6, were not smoothed. Visual inspection of the time trends in tabulated reflectance factor observations did not reveal serious discontinuities and the data were not smoothed; however, experiment means summarized in Figure 1c) and 1d) indicate that those measurements also contained experimental error.

In view of apprehensions about the data that also included interlocation variation in sun angle, soils, measurement instruments and technique, and possible leaf angle distributions, the display of the data in Figure 4 and the goodness of fits of the various equations in Tables 4, 5, and 6 for the pooled data from all locations are encouraging. Together they force the conclusion that the corn canopies, as characterized by the green leaf area index, strongly dominated the reflectance factor observations. Consequently, it was feasible to develop the generalized equations to recommend for predicting L of corn from spectral observations expressed as vegetation indices.

The equations given in Figure 4 or the power equations (29), (30), and (31) in Tables 4, 5, and 6 may be used for estimating L . In both cases the rank order from best to worst is GVI, PVI, NDVI, and RVI based on coefficients of determination, root mean square errors (RMSE), and robustness in fitting data from different instruments and experiments.

As shown by the RMSE associated with Eqs. (23) and (24) in Table 4, during the pre- L_{\max} period L could be estimated with a RMSE of 0.79 by NDVI and 0.49 by GVI. By comparison, the RMSE for estimating L from NDVI by Eq. (31) was 0.81 and by Eq. (28) was 0.85. Compared with the above, L could be estimated with a RMSE of 0.29 from LM [Eq. (40)].

A direct unconfounded comparison of instruments was possible in this study only for Tryon where Barnes Modular Multiband 12-1000 and Exotech 100 radiometers were both used on the same dates and close to the same times over the experimental plots. Figure 8 displays GVI calculated for these two instruments plotted against each other, the equation of the statistical fit, and the 1:1 line. The agreement between the two instruments was very close ($r^2 = 0.995$) and at $GVI = 20.9$ the two instruments agreed exactly. Thus, in the case of Tryon data at least the same conclusion would be reached whichever instru-

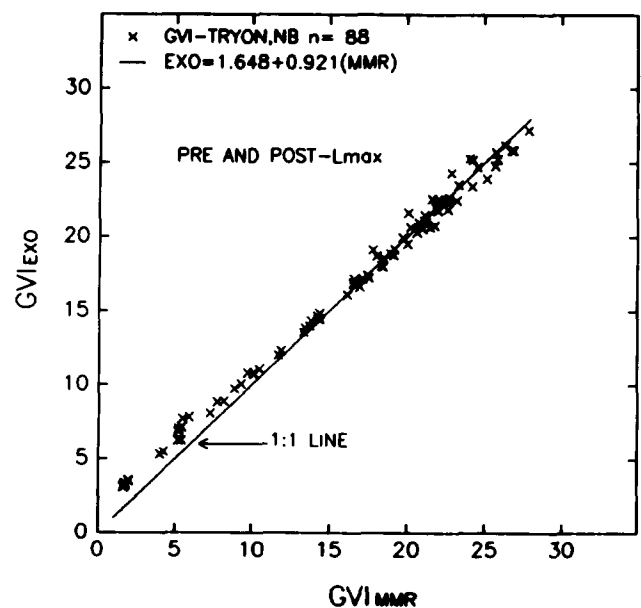


Figure 8. Comparison of GVI calculated from the Exotech (EXO) radiometer and the modular multiband radiometer (MMR) for Tryon.

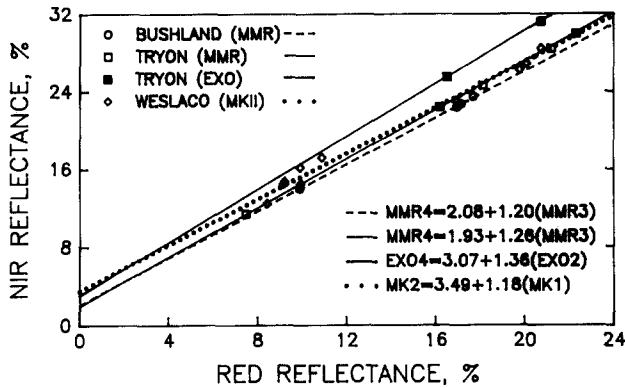


Figure 9. Comparison of soil lines by location and radiometer.

ment was used for the reflectance factor observations.

In Figure 4 it can be seen that the curves for GVI and NDVI coincided very closely when L was less than 2 whether the crop was developing or senescing, whereas, over the L range 0–2, the curves for NDVI and RVI are displaced by at least $0.5L$. GVI is referenced to a soil plane and PVI to a soil line and this improves their precision in estimating L at incomplete ground cover. Soil line equations given in Table 3 agreed well among locations and instruments as shown in Figure 9. The soil line for the Tryon EXO data falls above those for MMR and Mark II spectroradiometers because the midpoint of the NIR band (Table 2) for the Exotech instrument is higher ($0.95 \mu\text{m}$) than for the MMR and Mark II ($0.83 \mu\text{m}$) and soil reflectance increases with wavelength in the NIR. The good agreement among instruments is strong circumstantial evidence that instruments were not a strong source of variation in the data.

The careful reader will notice (Table 3) that a three-band greenness equation was used for the MMR data and a four-band greenness equation was used for the Exotech data for Tryon. The reason was that, for the Bushland data, the first three coefficients in the three- and four-band greenness equations were identical and the coefficient for the fourth band was 0.001. Consequently, they gave the same GVI. To be consistent within instruments across locations we used a three-band greenness for the Tryon MMR data also. For comparison, the four-band greenness equation for the Tryon MMR data was

$$\text{GVI} = -0.379(\text{MMR2}) - 0.647(\text{MMR2}) + 0.659(\text{MMR3}) + 0.061(\text{MMR5}). \quad (42)$$

Since the negative coefficients of the visible bands are within 0.03 of each other for three-band GVI in Table 3 and the four-band GVI above, and the sum of the positive coefficients for four-band greenness ($0.659 + 0.061$) is close to the 0.702 of the three-band greenness, the three-band and four-band GVI would also agree closely for the Tryon MMR data.

The three parameter model of Eq. (1) was included in this paper because it describes well the dependence of VI, FPAR, crop yield, and the reciprocal of canopy resistance to water vapor transfer ($1/r_c$) on leaf area index (Wiegand and Richardson, 1984; Sellers, 1985, 1987; Choudhury, 1987; Wiegand and Hatfield, 1988). All increase rapidly as L increases to 3 or 4, then approach a limiting value as L increases further.

The three parameters in Eq. (1) give it flexibility to uniquely describe individual treatments within experiments, and rather small differences in residual sums of squares associated with the various reduced forms of the model are significant by the F -test in among-location comparisons. Consequently, there are many equations and coefficients to summarize if applied to the number of treatments, experiments, and vegetation indices as characterized this study. The equations given in Tables 4 and 5 are the fully reduced form of the model expressed by Eq. (1); we judged them adequate for the among-location comparisons that we wanted to emphasize in this study.

However, the number of samples and the physical effort required to adequately sample crop, range, and forest stands for L (Daughtry and Hollinger, 1984; Curran and Williamson, 1986) cause users to want to estimate FPAR, $1/r_c$, plant dry matter, and economic yield from VI, which measure the amount of photosynthetically active tissue in the canopy (Wiegand et al., 1986) or the photosynthetic size of the canopy (Wiegand and Shibayama, 1989). Those relations are linear or nearly linear (Wiegand and Richardson, 1984; Sellers, 1987; Choudhury, 1987).

Users also want to estimate L from VI, a relation that is usually nonlinear. Therefore, the L and VI data from all locations were pooled and fit by linear, exponential, quadratic, and power equation forms by pre- L_{max} , post- L_{max} , and whole season portions (Tables 4, 5, and 6, respectively) to learn which equation form was best for each of the four vegetation indices considered. Careful com-

parison of the measures of goodness of fit showed that the power form equation described the two-band VI (PVI, NDVI, RVI) responses well, but that a quadratic or exponential form was better for the three- and four-band GVI.

REFERENCES

- Asrar, G., Fuchs, M., Kanemasu, E. T., and Hatfield, J. L. (1984), Estimating absorbed photosynthetically active radiation and leaf area index from spectral reflectance in wheat, *Agron. J.* 76:300–306.
- Best, R. G., and Harlan, J. C. (1985), Spectral estimation of green leaf area index of oats, *Remote Sens. Environ.* 17:27–36.
- Choudhury, B. J. (1987), Relationship between vegetation indices, radiation absorption, and net photosynthesis evaluated by sensitivity analysis, *Remote Sens. Environ.* 22:209–233.
- Curran, P. J., and Williamson, H. D. (1986), Sample size for ground and remotely sensed data, *Remote Sens. Environ.* 20:31–41.
- Daughtry, C. S. T., and Hollinger, S. E. (1984), Costs of measuring leaf area index of corn, *Agron. J.* 76:836–841.
- Dusek, D. A., and Musick, J. T. (1986), Spectral vegetation indices for estimating corn, sorghum, and wheat growth parameters, Paper No. 86-3575, Am. Soc. Agric. Eng.
- Dusek, D. A., Jackson, R. D., and Musick, J. T. (1985), Winter wheat vegetation indices calculated from combinations of seven spectral bands, *Remote Sens. Environ.* 18:255–267.
- Gallo, K. P., and Daughtry, C. S. T. (1986), Techniques for measuring intercepted and absorbed photosynthetically active radiation in corn canopies, *Agron. J.* 752–756.
- Gallo, K. P., Daughtry, C. S. T., and Bauer, M. E. (1985), Spectral estimation of absorbed photosynthetically active radiation in corn canopies, *Remote Sens. Environ.* 17:221–232.
- Goel, N. S. (1988), Models of vegetation canopy reflectance and their use in estimation of biophysical parameters from reflectance data, *Remote Sens. Rev.* 4:1–212.
- Hughes, A. P., and Freeman, P. R. (1967), Growth analysis using frequent small harvests, *Appl. Ecol.* 4:553–560.
- Jackson, R. D. (1983), Spectral indices in *n*-space, *Remote Sens. Environ.* 13:409–421.
- Jackson, R. D., and Moran, M. S. (1987), Field calibration of reference reflectance panels, *Remote Sens. Environ.* 22:145–158.
- Jackson, R. D., Slater, P. N., and Pinter, P. J., Jr. (1983), Discrimination of growth and water stress in wheat by various vegetation indices through clear and turbid atmospheres, *Remote Sens. Environ.* 13:187–208.
- Kauth, R. J., and Thomas, G. S. (1976), The Tasseled Cap—a graphic description of the spectral-temporal development of agricultural crops as seen by Landsat, in *Proc. Symp. Machine Processing of Remotely Sensed Data*, Purdue Univ., West Lafayette, IN, pp. 41–51.
- Maas, S. J., Richardson, A. J., Wiegand, C. L., and Nixon, P. R. (1985), Use of plant, spectral and weather data in modeling corn growth, in *Proc. 19th Int. Symp. Remote Sens. of Environ.* Univ. of Michigan, Ann Arbor, pp. 167–186.
- Redelfs, M. S., Stone, L. R., Kanemasu, E. T., and Kirkham, M. B. (1987), Greenness-leaf area index relationships for seven row-crops, *Agron. J.* 79:254–259.
- Rice, D. P., Crist, E. P., and Malila, W. A. (1980), Applicability of selected wheat remote sensing technology to corn and soybeans, Final Report No. 124000-9-F, Environ. Res. Inst. of Michigan, Ann Arbor.
- Richardson, A. J. (1981), Measurement of reflectance factors under daily and intermittent irradiance variations, *Appl. Opt.* 20: 3336–3340.
- Richardson, A. J. and Wiegand, C. L. (1977), Distinguishing vegetation from soil background information, *Photogramm. Eng. Remote Sens.* 43:1541–1552.
- Robinson, B. F., Bauer, M. E., De Witt, D. P., Silva, L. F., and Vanderbilt, V. C. (1979), Multiband radiometer for field research, *SPIE* 196:8–15.
- Rouse, J. W., Jr., Haas, R. H., Schell, J. A. and Deering, D. W., (1974), Monitoring vegetation systems in the Great Plains with ERTS, Third ERTS Sympos., I:309–317, NASA SP-351, U.S. Govt. Printing Office, Washington, D.C.
- SAS Institute Inc. (1988), *SAS/STATTM User's Guide*, Release 6.03 Edition, Cary, NC.
- Sellers, P. J. (1985), Canopy reflectance, photosynthesis, and transpiration, *Int. J. Remote Sens.* 6:1335–1372.
- Sellers, P. J. (1987), Canopy reflectance, photosynthesis, and transpiration. II. The role of biophysics in the linearity of their interdependence, *Remote Sens. Environ.* 21:143–183.
- Shibayama, M. and Akiyama, T. (1989), Seasonal visible and near-infrared spectra of rice canopies in relation to LAI and above-ground dry mass, *Remote Sens. Environ.* 27:119–127.
- Tucker, C. J. (1979), Red and photographic-infrared linear combinations for monitoring vegetation, *Remote Sens. Environ.* 8:127–150.
- Tucker, C. J., Jones, W. H., Kley, N. A., and Sundstrom, G. J. (1981), A three-band hand-held radiometer for field use, *Science* 211: 281–283.
- Verhoef, W. (1984), Light scattering by leaf layers with application to canopy reflectance modeling: The SAIL model, *Remote Sens. Environ.* 16:125–141.

- Wanjura, D. F., and Hatfield, J. L. (1988), Vegetative and optical characteristics of four-row crop canopies, *Int. J. Remote Sens.* 9:249–258.
- Wiegand, C. L., and Hatfield, J. L. (1988), The spectral-agronomic multisite-multicrop analyses (SAMMA) project, *Int. Arch. Photogramm. Remote Sens.* 27(B7):696–706.
- Wiegand, C. L., and Richardson, A. J. (1984), Leaf area, light interception, and yield estimates from spectral components analysis, *Agron. J.* 76:543–548.
- Wiegand, C. L., and Richardson, A. J. (1987), Spectral components analysis: rationale and results for three crops, *Int. J. Remote Sens.* 8:1011–1032.
- Wiegand, C. L., Shibayama, M., Yamagata, Y., and Akiyama, T. (1989), Spectral observations for estimating the growth and yield of rice, *Jap. J. Crop Sci.* 58:673–683.